Stability of hydrocarbons at deep Earth pressures and temperatures

Leonardo Spanu[a,1], Davide Donadio[a,b], Detlef Hohl[c], Eric Schwegler[d], and Giulia Galli[a,e]

[a]Department of Chemistry, University of California, Davis, CA 95616; [b]Max Planck Institute for Polymer Research, Ackermannweg 10, 55128 Mainz, Germany; [c]Shell Global Solutions, 3737 Bellaire Boulevard, Houston, TX 77025; [d]Lawrence Livermore National Laboratory, Livermore, CA 94551; and [e]Department of Physics, University of California, Davis, CA 95616

Edited by Russell J. Hemley, Carnegie Institution of Washington, Washington, DC, and approved March 18, 2011 (received for review October 4, 2010)

Determining the thermochemical properties of hydrocarbons (HCs) at high pressure and temperature is a key step toward understanding carbon reservoirs and fluxes in the deep Earth. The stability of carbon-hydrogen systems at depths greater than a few thousand meters is poorly understood and the extent of abiogenic HCs in the Earth mantle remains controversial. We report ab initio molecular dynamics simulations and free energy calculations aimed at investigating the formation of higher HCs from dissociation of pure methane, and in the presence of carbon surfaces and transition metals, for pressures of 2 to 30 GPa and temperatures of 800 to 4,000 K. We show that for $T \geq 2{,}000$ K and $P \geq 4$ GPa HCs higher than methane are energetically favored. Our results indicate that higher HCs become more stable between 1,000 and 2,000 K and $P \geq 4$ GPa. The interaction of methane with a transition metal facilitates the formation of these HCs in a range of temperature where otherwise pure methane would be metastable. Our results provide a unified interpretation of several recent experiments and a detailed microscopic model of methane dissociation and polymerization at high pressure and temperature.

carbon cycle | Earth interior | numerical simulation

There is growing evidence that carbon-bearing compounds in the deep Earth contribute to the global carbon cycle (1, 2). We have limited knowledge of the role played by pressure and temperature on reactions in the C-O-H system under these conditions. In the case of methane, many open questions remain concerning its dissociation and possible polymerization under pressure, in spite of several experiments carried out in recent years (3–6).

Laboratory experiments indicate that methane can form under P-T conditions of the Earth's upper mantle through carbonate reduction processes (7). For $T > 1{,}000$ K and $P = 4$–5 GPa, thermochemical models (8) predict that methane is less stable than complex mixtures of hydrocarbons (HCs) (e.g., ethane, propane, etc.), although there is no general consensus on the temperature and pressure conditions at which dissociation and polymerization processes begin. Experiments have not yet probed the microscopic mechanisms leading to dehydrogenation of methane under pressure and formation of higher hydrocarbons.

Laser-heated diamond anvil cell (DAC) experiments (3) indicate the formation of both HCs and diamond at 19 GPa and 2,000–3,000 K. These results are consistent with those of shock compression studies (9), suggesting dissociation of methane and diamond formation at 20 GPa and 2,000 K. Recent Raman measurements (6) support the formation of ethane, propane, and butane upon methane compression, in a range of pressure and temperature compatible with upper mantle conditions, i.e., $P \simeq$ 2–5 GPa and $T \simeq 1{,}000$–$1{,}500$ K. Ethane was also found as a reaction product in a DAC experiment (5) at $T > 1{,}100$ K and $P > 10$ GPa. All experimental results to date indicate that heavier hydrocarbons form upon compression of methane (3–6).

To investigate the relative stability of methane and higher HCs and provide a microscopic picture of the high P-T formation of the latter, we have carried out a series of ab initio molecular dynamics (MD) simulations and free energy calculations of pure methane and mixtures of ethane and molecular hydrogen. We have also simulated methane in the presence of Ir to understand the effect of metals on the polymerization process, and we have investigated the interaction of compressed methane with diamond surfaces and graphite to mimic several chemical environments in the Earth.

The duration of our ab initio simulations is limited to tens of picoseconds, and therefore only at high T (specifically $T \geq 4{,}000$ K) could we use direct simulations to observe dissociation processes and dehydrogenation. At lower T, we carried out free energy calculations to study the relative stability of methane and hydrocarbon mixtures. We start by describing the results of ab initio MD simulations at 4,000 K. Although such a temperature is not relevant to upper mantle processes, calculations under these conditions allowed us to study the role of pressure when dissociation phenomena are readily observed. As illustrated in Fig. 1, our MD simulations of pure methane show the spontaneous formation of complex HCs over a wide range of pressures at $T = 4{,}000$ K. The formation of molecular hydrogen, ethylene, ethane, and propane is observed over a moderate pressure range ($P = 2$–4 GPa). For P larger than 12 GPa, HCs with longer chains and seeds of sp^2-bonded clusters begin to appear (Fig. 1*B*, Fig. 2*A*). Signatures of C-C bonds can be identified, for example, in the computed vibrational density of states (VDOS) obtained at 12 GPa (see Fig. 2), where we find a noticeable feature at 1,600 cm^{-1} that originates from small clusters of threefold coordinated carbon atoms in graphite-like configurations. A similar peak is present in the computed VDOS at lower pressure, but arises from the C-C stretching mode of ethylene molecules (C_2H_4). In the entire pressure range examined here, we did not find any evidence for the formation of diamond-like clusters (10, 11). Our simulations at 4,000 K indicate that once dehydrogenation occurs, methane polymerization is favored by an increase of pressure.

Our simulations of pure methane carried out at 1,000, 2,000, and 3,000 K did not show any dissociation and thus any formation of high HCs, possibly because of their duration (about 10 ps). Therefore, to investigate the stability of longer alkanes we performed enthalpy and entropy calculations. In particular, we compared the free energies of methane with ethane (C_2H_6) and propane (C_3H_8), the main reaction products of methane polymerization observed in DAC experiments (5, 6). We considered the reactions $CH_4 \rightarrow 1/n\ C_nH_{2n} + 2 + (n-1)/nH_2 (n \geq 2)$, and we performed constant volume and energy (NVE) simulations of methane and of mixtures of ethane and hydrogen, and propane

Author contributions: L.S. designed the research, performed simulations, analyzed data, discussed results, and wrote the paper; D.D. helped setting up simulations, discussed results, and reviewed the manuscript; E.S., D.H. discussed results and reviewed the manuscript; and G.G. designed the research, discussed results, and wrote the paper.

The authors declare no conflict of interest.

This article is a PNAS Direct Submission.

Freely available online through the PNAS open access option.

[1]To whom correspondence should be addressed. E-mail: lspanu@ucdavis.edu.

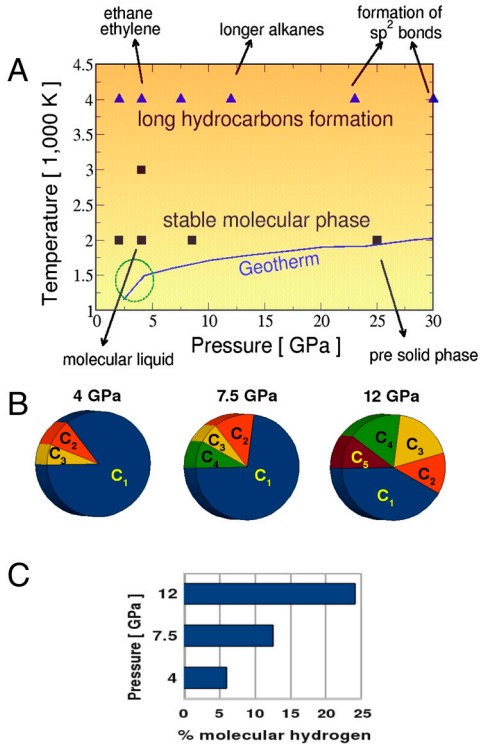

Fig. 1. Results from ab initio MD simulations. (*A*) Methane and hydrocarbon products found in our ab initio MD simulations of pure fluids (no metals or carbon surfaces present), as a function of pressure and temperature. Black squares indicate pressure-temperature conditions where pure methane does not dissociate in direct ab initio MD simulations. Blue filled triangles represent conditions where formation of hydrocarbons is observed in our simulations. The solid blue curve indicates the Earth mantle geotherm. The dashed green circle identifies the experimental P-T condition achieved in ref. 6 where formation of hydrocarbons from methane was detected in DAC experiments with absorbers. (*B*) Chart diagrams of carbon products found in our simulations at 4, 7.5, and 12 GPa, at 4,000 K. C_n ($n = 1,5$) indicates the number of carbon atoms in the final products. (*C*) Percentage of hydrogen in molecules found at 4, 7.5, and 12 GPa, at 4,000 K.

and hydrogen, for a fixed C-H composition. Our simulations were carried out at 1,000 K and 2 GPa and 2,000 K and 4 and 8 GPa. The P-T range was chosen so as to be representative of upper mantle conditions and to be related to the conditions achieved in recent DAC experiments (Fig. 3).

After equilibrating the volume at a given pressure, we used our computed average volume and total energies to obtain the enthalpies of the liquid. From velocity-velocity autocorrelation functions we evaluated vibrational contributions to the free energy and we computed the entropies of the molecular fluids following the method proposed in ref. 12 (see *Materials and Methods*). Our results are summarized in Table 1 and Table 2. In Table 1 we report the enthalpy and entropy differences for the reaction $CH_4 \rightarrow 1/3C_3H_8 + 2/3H_2$ and $CH_4 \rightarrow 1/2C_2H_6 + 1/2H_2$. Table 2 lists the rotational, vibrational, and translational components of the entropy. We note that at 2,000 K the entropic contribution to the free energy difference is nearly constant, as P is varied from 4 to 8 GPa.

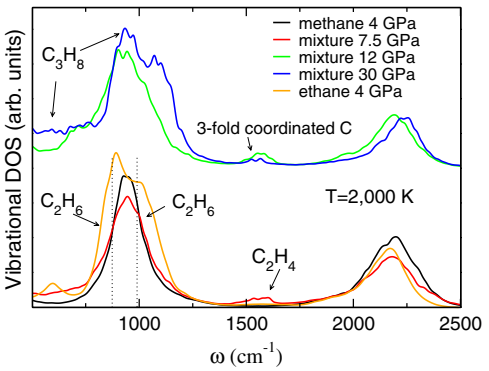

Fig. 2. Vibrational spectra. Computed carbon vibrational density of state for pure methane (black line), ethane (orange line), and hydrocarbons mixtures at 7.5 GPa (red line), 12 GPa (green line), and 30 GPa (blue line) at T = 2,000 K. Alkane mixtures were prepared by annealing configurations generated with MD simulations at 4,000 K.

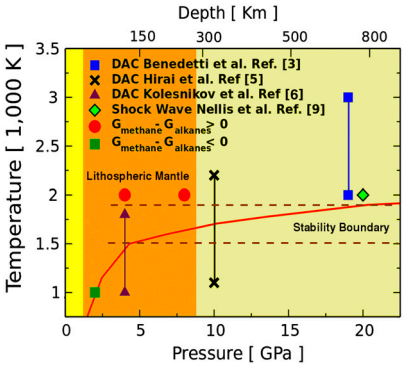

Fig. 3. Proposed boundaries for methane stability. Temperature boundaries for methane stability are indicated by dashed lines. Green square and red dots indicate the results of our free energy calculations (see Table 1). At 4 GPa and T < 2,000 K, the entropies of liquid methane and of the mixtures were estimated by using atomic velocities rescaled from those computed at 2,000 K. Experimental points denote the lowest pressure and temperature points at which hydrocarbon formation was observed. The solid red line represents P-T conditions along the Earth geotherm. Conditions in the lithospheric mantle correspond approximately to the region highlighted in orange.

Our calculations at 1,000 and 2,000 K show that enthalpic terms favor the stability of pure methane, whereas entropic effects help stabilize heavier HCs. At 2,000 K and 4 and 8 GPa, the mixture of ethane and molecular hydrogen is energetically favored with respect to methane (Table 1 and Table 2). At 1,000 K and 2 and 4 GPa the entropic contributions do not compensate the enthalpy difference between methane and ethane (and propane), and methane is more stable than mixtures of higher HCs. These results indicate that between 1,000 and 2,000 K and P ≥ 4 GPa, corresponding to depths of >120 km, mixtures of heavier HCs and hydrogen become more stable than methane. Our proposed P-T boundaries for methane stability are in good agreement with experimental results as summarized in Fig. 3. In a recent experiment described in ref. 5, the signature of C-C bonds appears between 1,100 and 2,200 K and it becomes clearly evident for T > 1,800 K. In ref. 6, HCs are detected in the range from 1,000 to 1,500 K and P > 2 GPa. Because the formation of heavier HCs from methane is largely driven by entropy,

Table 1. Enthalpy (ΔH) and entropy (ΔS) differences per carbon atom (eV) of C-H systems with respect to methane, at different P-T conditions

	ΔH	$-T\Delta S$	ΔG
$T = 1{,}000$ K; $P = 2$ GPa			
$CH_4 \rightarrow 1/2\ C_2H_6 + 1/2\ H_2$	0.46(3)	−0.15(9)	0.31(0.12)
$CH_4 \rightarrow 1/3\ C_3H_8 + 4/3\ H_2$	0.57(3)	−0.32(9)	0.25(0.12)
$T = 2{,}000$ K; $P = 4$ GPa			
$CH_4 \rightarrow 1/2\ C_2H_6 + 1/2\ H_2$	0.41(5)	−0.53(5)	−0.11(0.1)
$T = 2{,}000$ K; $P = 8$ GPa			
$CH_4 \rightarrow 1/2\ C_2H_6 + 1/2\ H_2$	0.35(5)	−0.52(6)	−0.17(0.1)

$\Delta H = H_{mixture} - H_{methane}$ and $-T\Delta S = -T(S_{mixture} - S_{methane})$

Table 2. Rotational, vibrational, and translational contributions to the entropic term $-T\Delta S$ for liquid methane and a mixture of ethane and hydrogen, at $T = 2{,}000$ K and $P = 4$ GPa

-TS (eV)	Rotation	Vibration	Translation	Total
Methane	−26.5(2)	−78.5(1)	−94.0(7)	−199(1)
Ethane	−20.3(1)	−99.5(1)	−50.5(4)	−170.3(6)
Hydrogen	−7.6(5)	−5.7(1)	−41.1(3)	−54.4(9)
$-T\Delta S/CH_4$	−0.02(2)	−0.55(3)	0.04(2)	−0.53(5)

T is the temperature and S is the entropy

methane polymerization is more sensitive to temperature than to pressure changes.

To further understand the stability and dissociation of compressed methane, we have carried out a series of simulations of the liquid in contact with an Ir_4 cluster at a pressure of 4 GPa and temperatures of 800, 1,500, and 2,500 K. The motivation for such a computational experiment is twofold. In a number of industrial low-P processes, the breaking of C-H bonds is catalyzed by the use of noble metals (13). In addition, in laser-heated DAC experiments it is common practice to include a coupler (often a noble metal) to absorb the laser energy and heat the sample (3, 5, 6). Liquid methane is optically transparent, and thus it is not feasible to directly heat methane with the typical laser beam used in these experiments. Experiments with metal Ir (5, 6) and nonmetal absorbers (Boron) (6) yielded the same final reaction products. Nevertheless, the effect of an absorber/methane interface on the reaction dynamics remains to be understood.

The highest temperature reached in the above laser heating experiments is reported to be about 2,500 K (5, 6). Considering that the melting temperature of Ir is ≃2,719 K (14) at ambient pressure, and that temperature fluctuations may be present in the laser spot, one can expect the Ir surface to be slightly disordered and defective at 2,500 K. An Ir_4 cluster is a reasonable model of highly reactive sites (15) present on the surface of the plate or powders used in a DAC experiment. When Ir is introduced into our MD cell, methane readily dissociates. Because of the high diffusivity of the fluid, at 2,500 K several dissociation events are observed, together with recombination of H and CH_3 groups in molecular hydrogen and ethane (Fig. 4*A*). Our simulations suggest that in DAC experiments with metal absorbers molecular hydrogen and alkanes are formed in the laser-heated region where methane is in contact with the Ir metal, consistent with the results of refs. 5 and 6. Even at temperatures as low as 800 K, we observe methane dissociation at 4 GPa in our simulations in the presence of Ir_4. At this T the fragments –H and CH_3–

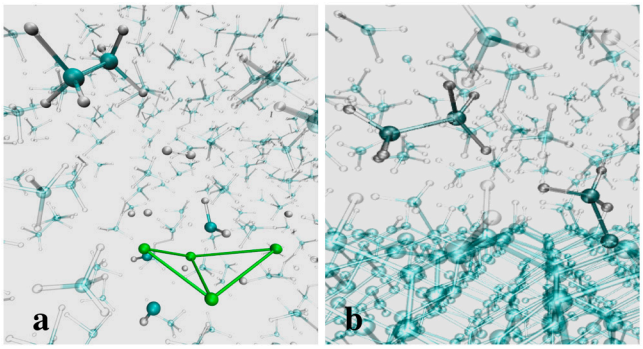

Fig. 4. Snapshots from ab initio simulations. (*A*) Methane in contact with an Ir_4 cluster at 2,500 K and 4 GPa: The Ir_4 cluster acquires a butterfly shape and several fragments—CH_3 and CH_2—are observed during the simulation together with molecular hydrogen and ethane. (*B*) Liquid methane in contact with a partially H-terminated diamond surface [100] at 2,500 K and P ≈ 4 GPa. A CH_3 group attached to the surface and a newly formed ethane molecule are highlighted.

bind to the Ir_4 cluster for several picoseconds, preventing us from studying whether subsequent formation of ethane and hydrogen occurs or methane is reformed. These findings, combined with our free energy calculations, indicate that the metal acts as a catalyst facilitating the dehydrogenation and then the polymerization of pure methane. Therefore our calculations suggest that the use of an Ir coupler (and most likely other noble metals as well) in DAC experiments affects the kinetic of the polymerization reaction. We emphasize that in the absence of a metal, our direct MD simulations at 2,000 K do not show the formation of HCs, and methane remains in a metastable state for pressure up to 24 GPa. These results are consistent with infrared measurements reported in ref. 16 showing that methane is metastable well above 100 GPa, in the absence of heating. They are also consistent with the DAC experiment reported in ref. 5 showing that for T < 1,100 K methane remains in a molecular state for pressure up to 81 GPa.

Under deep Earth conditions, C-H fluids may come in contact with graphitic carbon or diamond (17). At low-P, for industrial applications the methane-carbon interaction has been investigated as a pathway for hydrogen production (18, 19). For example, at atmospheric pressure and temperatures between 1,023 and 1,173 K methane is known to react with coal (lignite, anthracite) forming molecular hydrogen, carbon [predominantly in graphite-like forms (20)] and a small amount of hydrocarbons (0.1%) (18). The active sites for the dehydrogenation mechanism have been identified as defects at the surface (19, 21). An increase in the chemical activity of C-H-O fluids was also observed in recent DAC experiments at upper mantle conditions (22) in the presence of graphite. Sharma et al. (22) reported that the presence of graphite enhances the formation of methane from C-H-O fluids (starting from formic acid), and hydrocarbons were detected as a possible back reaction.

We simulated liquid methane in contact with a diamond surface reconstructed in the [100] direction and partially covered with hydrogen. We performed calculations at 1,500 K and 2,500 K and at P ≃ 4 GPa. When a methane molecule approaches an unsaturated C atom at the diamond surface, it spontaneously dissociates and a CH_3 radical forms in the fluid. CH_3 groups can then either bond with an unsaturated surface atom or combine to form ethane. In Fig. 4*B* we show a snapshot of a simulation of a diamond surface in contact with compressed methane at 2,500 K where an ethane molecule and a CH_3 group on the surface are clearly visible. The temperature of diamond surfaces in DAC experiments is estimated to be lower than the one simulated here, that is 300–400 K, based on a simplified model of thermal transport inside the DAC chamber (23). However much refined models are needed to establish the temperature at the diamond surface. Our results suggest that hot spots in laser-heated DAC may be regions where methane dissociation is more easily started. Finally, we investigated methane in contact with an unsaturated fragment of graphite. During a simulation at 1,500 K we observed dissociation of methane molecules, induced by reactions with unsaturated carbon atoms. We did not observe formation of molecular hydrogen or longer alkanes, probably because of our short simulation time (several picoseconds). Our results support the hypothesis that interaction with carbon surfaces may lead to the dissociation of methane and to the formation of CH_3 and CH_2 groups in the fluid at upper mantle P-T conditions at a depth greater than ≈120 km.

In summary, we have investigated the formation of heavier alkanes from methane for temperature up to 4,000 K and pressure between 2 and 30 GPa using ab inito MD simulations and free energy calculations. We have shown that between 1,000 and 2,000 K and P ≥ 4 GPa mixtures of longer HCs and hydrogen are thermodynamically more stable than methane. These P-T conditions correspond to depths greater than 120 km. At these conditions, we found that the interaction with a noble metal facilitates

methane dissociation and polymerization reactions. In contrast without the catalytic effect of the metal, direct MD simulation of methane shows no dissociation for temperatures up to 4,000 K, possibly indicating its metastability. Formation of hydrocarbons between 1,500 and 2,500 K is also observed when methane interacts with unsaturated diamond surfaces. Our results indicate that the formation of higher hydrocarbons from pure methane is likely to occur when carbon-bearing fluids are in contact with metals or solid carbon phases. On the other hand, the extent of free elemental carbon at depth in the Earth is not known (see Deep Carbon Observatory, https://dco.gl.ciw.edu/).

Because of the observed metastability of methane in our MD simulations, one may speculate that at upper mantle conditions methane is metastable and it may exist together with higher hydrocarbons that have a lower free energy. The relative concentration of methane and higher HCs depends on the environment, e.g., available interfaces with carbon deposits and/or transition metal surfaces.

Materials and Methods

We have carried out ab initio MD simulations in the Born–Oppenheimer approximation using the Qbox code (24). Pure methane was simulated in a cell with 48 molecules. The simulated ethane and molecular hydrogen mixture contained 24 ethane and 24 hydrogen molecules. The simulated propane and molecular hydrogen mixture contained 16 propane and 32 hydrogen molecules. For diamond-methane simulations we used 24 methane molecules and a diamond slab (in the [100] direction) with four diamond layers for a total of 64 carbon atoms in the diamond geometry. For the Ir-methane system we simulated four Ir atoms and 48 methane molecules. In our ab initio MD we substituted hydrogen with deuterium for computational convenience, so as to use a larger time step (5 a.u.) when integrating the Newton equations of motion. For all the systems investigated here we used a cubic supercell and the gamma point only to sample the supercell Brillouin zone. We used the Perdew–Burke–Ernzerhof (25), generalized gradient corrected approximation, for the exchange and correlation functional, norm conserving pseudopotentials and a plane-wave expansion of the Kohn–Sham orbitals with a kinetic-energy cutoff of 60 Rydberg (Ry). As a test of the accuracy of the functional, we estimated the free energy difference of methane and a hydrogen and ethane mixture at zero pressure, using the frequencies calculated for the gas phase. At 1,000 K we obtained a free energy difference per carbon atom of 0.27 eV to be compared with 0.36 eV given in ref. 8. All the pressure values were corrected for basis set noncompleteness by calculating the stress for selected configurations with a cutoff of 200 Ry. All the systems were equilibrated for about 4 ps in the constant pressure and temperature ensemble. After equilibration, constant volume and temperature simulations were performed over a time of about 10 ps per MD run. Entropies were calculated using the two-phase thermodynamic model introduced in ref. 12. The method is based on the separation of the density of vibrational states (DOS) into diffusive and nondiffusive terms. Such separation is performed for intermolecular vibrations, rotations, and translations. The DOS were computed from velocity-velocity autocorrelation functions (Fig. 3*B*) of an NVE trajectory over a time of at least 10 ps.

ACKNOWLEDGMENTS. We thank V.G. Kutcherov (Royal Institute of Technology), A.F. Goncharov (Geophysical Laboratory, Carnegie Institution of Washington), H. Kuipers (Shell Global Solutions), and D. Foustoukos (Geophysical Laboratory, Carnegie Institution of Washington) for a critical reading of the manuscript and for useful discussions. We also acknowledge useful discussions with F. Gygi (University of California, Davis) and P. Giaquinta (University of Messina). Calculations were performed at the Lawrence Livermore National Laboratory and at the University of California Shared Computer Center on the Mako cluster. This work was supported by a grant from Stichting Shell Research.

1. Heimann M, Reichstein M (2008) Terrestrial ecosystem carbon dynamics and climate feedbacks. *Nature* 451:289–292.
2. Fischer TP, et al. (2009) Upper-mantle volatile chemistry at oldoinyo lengai volcano and the origin of carbonatites. *Nature* 459:77–80.
3. Benedetti LR, et al. (1999) Dissociation of CH_4 at high pressures and temperatures: Diamond formation in giant planet interiors? *Science* 286:100–102.
4. Zerr A, Serghiou G, Boehler R, Ross M (2006) Decomposition of alkanes at high pressures and temperatures. *High Pressure Res* 26:23–32.
5. Hirai H, Konagai K, Kawamura T, Yamamoto Y, Yagi T (2009) Polymerization and diamond formation from melting methane and their implications in ice layer of giant planets. *Phys Earth and Planet Inter* 174:242–246.
6. Kolesnikov A, Kutcherov VG, Goncharov AF (2009) Methane-derived hydrocarbons produced under upper-mantle conditions. *Nat Geosci* 2:566–570.
7. Scott HP, et al. (2004) Generation of methane in the Earth's mantle: In situ high pressure-temperature measurements of carbonate reduction. *Proc Natl Acad Sci USA* 101:14023–14026.
8. Kenney JF, Kutcherov VA, Bendeliani NA, Alekseev VA (2002) The evolution of multicomponent systems at high pressures: VI. The thermodynamic stability of the hydrogen-carbon system: The genesis of hydrocarbons and the origin of petroleum. *Proc Natl Acad Sci USA* 99:10976–10981.
9. Nellis WJ, Ree FH, Vanthiel M, Mitchell AC (1981) Shock compression of liquid carbon-monoxide and methane to 90 GPa (900 kbar). *J Chem Phys* 75:3055–3063.
10. Ancilotto F, Chiarotti G, Scandolo S, Tosatti E (1997) Dissociation of methane into hydrocarbons at extreme (planetary) pressure and temperature. *Science* 275:1288–1290.
11. Ghiringhelli LM, et al. (2008) State-of-the-art models for the phase diagram of carbon and diamond nucleation. *Mol Phys* 106:2011–2038.
12. Lin ST, Maiti PK, Goddard WA, III (2010) Two-phase thermodynamic model for efficient and accurate absolute entropy of water from molecular dynamics simulations. *J Phys Chem B* 114:8191–8198.
13. Enger BC, Lodeng R, Holmen A (2008) A review of catalytic partial oxidation of methane to synthesis gas with emphasis on reaction mechanisms over transition metal catalysts. *Appl Catal A Gen* 346:1–27.
14. Bedford RE, Bonnier G, Maas H, Pavese F (1996) Recommended values of temperature on the international temperature scale of 1990 for a selected set of secondary reference points. *Metrologia* 33:133–154.
15. Engstrom JR, Goodman DW, Weinberg WH (1986) Hydrogenolysis of n-butane over the (111) and (110)-(1x2) surfaces of iridium—a direct correlation between catalytic selectivity and surface-structure. *J Am Chem Soc* 108:4653–4655.
16. Hemley RJ, Mao HK (2004) New findings in the static high-pressure science. *AIP Conf Proc* 706:17–26.
17. Holloway JR (1984) Graphite-CH_4-H_2O-CO_2 equilibria at low-grade metamorphic conditions. *Geology* 12:455–458.
18. Bai ZQ, Chen HK, Li W, Li BQ (2006) Hydrogen production by methane decomposition over coal char. *Int J Hydrogen Energy* 31:899–905.
19. Muradov N, Smith F, T-Raissi A (2005) Catalytic activity of carbons for methane decomposition reaction. *Catal Today* 102:225–233.
20. Muradov N (2001) Hydrogen via methane decomposition: An Application for decarbonization of fossil fuels. *Int J Hydrogen Energy* 26:1165–1175.
21. Huang L, Santiso EE, Nardelli MB, Gubbins KE (2008) Catalytic role of carbons in methane decomposition for co- and co_2-free hydrogen generation. *J Chem Phys* 128:214702–214709.
22. Sharma A, Cody GD, Hemley RJ (2009) In situ diamond-anvil cell observations of methanogenesis at high pressures and temperatures. *Energ Fuel* 23:5571–5579.
23. Kiefer B, Duffy TS (2005) Finite element simulations of the laser-heated diamond-anvil cell. *J Appl Phys* 97:114902.
24. Gygi F (2008) Architecture of Qbox: A scalable first-principles molecular dynamics code. *IBM J Res Dev,* 52 pp:137–144, Available at http://eslab.ucdavis.edu/software/qbox/index.htm.
25. Perdew JP, Burke K, Ernzerhof M (1996) Generalized gradient approximation made simple. *Phys Rev Lett* 77:3865–3869.